DOI: 10.1002/anie.201007047

Energetic Materials

Experimental Detection of Trinitramide, $N(NO_2)_3$**

Martin Rahm, Sergey V. Dvinskikh, István Furó, and Tore Brinck**

There is an incentive for research directed towards new environmentally friendly oxidizers and energetic materials.[1–3] Recent examples for advances in polynitrogen chemistry are the bulk synthesis of the V-shaped N_5^+,[4,5] the tetrazole-based CN_7^-,[6] and the detection of cyclic N_5^-.[7,8] Compounds containing exclusively oxygen and nitrogen are desirable for applications such as environmentally benign rocket propulsion. Of those, the dinitramide anion ($N(NO_2)_2^-$)[9–11] is the heaviest compound known to date.

Trinitramide (TNA; $N(NO_2)_3$) constitutes a possible energetic green oxidizer that could be suitable for future high-performance propellants. Only a few theoretical works have previously dealt with this hitherto unknown nitrogen oxide.[12–14] The heat of formation ($\Delta H^0_{f(gas)}$) of TNA has been estimated at between 38 and 71 kcal mol^{-1},[12–14] and the N–N bond dissociation energy has been estimated to be 20–27 kcal mol^{-1}.[13,14] The existence of an N_4O_6 intermediate has also been speculated to explain observed decomposition kinetics of dinitraminic acid ($HN(NO_2)_2$) in nitric acid.[15] To the best of our knowledge, no synthetic effort toward TNA has been attempted. Herein we present the first experimental detection of this exotic molecule.

We initially subjected TNA to a thorough quantum chemical analysis. The aim of this study was to decipher the kinetic stability and different decomposition pathways in gas phase and in solution. We also performed calculations on two possible synthesis routes, and estimated physical properties such as density, heat of formation, vaporization, sublimation, and performance characteristics of TNA as a rocket-propellant component.

Proposed self-decomposition pathways available to TNA are shown in Scheme 1. The N–N bond dissociation enthalpy in the gas phase is calculated to be 28.2 kcal mol^{-1}. Owing to the favorable change in entropy, this dissociation is likely the dominant route for decomposition in the gas phase. The transition state **TS1** (Scheme 1) was found to be in close competition with the homolytic bond fission, with a barrier corresponding to a relative free energy of 27.9 kcal mol^{-1}.

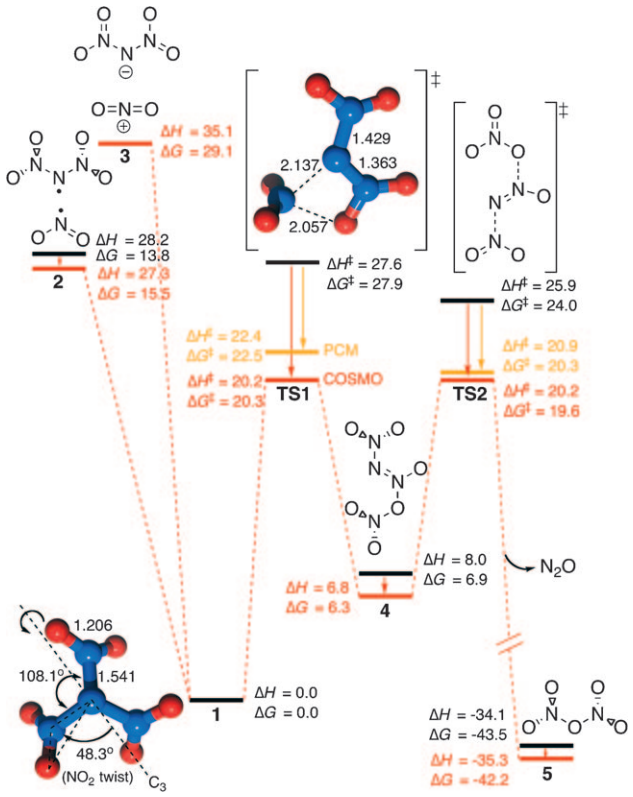

Scheme 1. The potential-energy surface surrounding TNA (**1**) investigated at the CBS-QB3 level of theory (energies [kcal mol^{-1}], bond lengths [Å]). Black and colored lines correspond to gas-phase (1 atm) and THF solution (1 M), respectively.

Surprisingly, DFT methods, such as the widely used B3LYP, or the more recent B2PLYP functional, fail in describing the energy landscape of both these pathways. The barrier heights are underestimated by 8–11 kcal mol^{-1} compared to CBS-QB3 (extrapolated CCSD(T)) and SCS-MP2 calculations, which are in very good agreement. As we know from previous studies that B3LYP, B2PLYP, and high-level ab initio methods (such as CCSD(T) and SCS-MP2) behave very similarly when treating $N(NO_2)_2^-$ and its radical,[16] and, given the high accuracy of the latter methods, we can safely assume that the error by DFT stems from an overestimation of the TNA ground state energy. Thus, the limited interest in TNA might be caused by the wide use of B3LYP, which underestimates its stability.

The character of **TS1** is between a NO_2 radical and a NO_2 cation transfer, with an increased importance of the latter in

[*] Dr. M. Rahm, Dr. S. V. Dvinskikh, Prof. I. Furó, Prof. T. Brinck
Physical Chemistry, School of Chemical Science and Engineering
Royal Institute of Technology (KTH)
100 44 Stockholm (Sweden)
Fax: (+46) 8-790-8207
E-mail: martinr@kth.se
tore@physchem.kth.se
Dr. M. Rahm
Competence Centre for Energetic Materials (KCEM)
Gammelbackavägen 6, 69151 Karlskoga (Sweden)

[**] We gratefully acknowledge support given by the Swedish Research Council (VR), the Swedish Defence Research Agency (FOI), and Eurenco Bofors. Exselent and the Knut and Alice Wallenberg foundation are thanked for the IR equipment. Michael Holmboe, Madeleine Warner, and Henrik Skifs are thanked for their kind assistance.

Supporting information for this article is available on the WWW under http://dx.doi.org/10.1002/anie.201007047.

solvated media. There is therefore a large solvent effect on the activation barrier. In a low-polarity solvent, the free-energy barrier for **TS1** is estimated to be only 20–23 kcal mol^{-1}, depending on solvation method. Thus, compared to homolytic (**1**→**2**) and heterolytic (**1**→**3**) bond fission, passage over **TS1** is clearly the dominant decomposition pathway in solution. Based on the assumed first-order decomposition kinetics, TNA should exhibit a half-life of roughly 10 days at −40 °C, or 230 years at −80 °C.

The initial decomposition products of TNA are predicted to be NO_2, N_2O, and NO_3 gas, which are produced by the rupture of conformer **4** through **TS2** (Scheme 1). NO_2 and NO_3 are expected to combine into dinitrogen pentoxide (N_2O_5; **5**), which in turn is in equilibrium with its ionic constituents NO_2^+ and NO_3^-. HNO_3 is likely to be generated through subsequent hydrogen abstraction reactions involving NO_3, protonation of NO_3^-, and hydrolysis of NO_2^+.

It has been demonstrated that the variation of the electrostatic potential (ESP) over the molecular surface can be correlated to several macroscopic properties reflecting intermolecular interaction tendencies, such as lattice enthalpy, heat of sublimation, and boiling point.[17,18] We have estimated the heat of vaporization ($\Delta H_{vap} \approx 7.8$ kcal mol^{-1}) and sublimation ($\Delta H_{sub} \approx 6.6$ kcal mol^{-1}) of TNA from its computed surface ESP. On the basis of comparisons with a range of other compounds, such as tetranitromethane ($\Delta H_{vap} = 11.9$ kcal mol^{-1}, $T_m = 13.8$ °C), trinitromethane ($\Delta H_{vap} = 13.1$ kcal mol^{-1}, $T_m = 15$ °C), and benzene ($\Delta H_{vap} = 8.0$ kcal mol^{-1}, $T_m = 5.5$ °C), we predict pure TNA to be in liquid form close to ambient temperatures, where it will decompose rapidly.

The solid-state density of TNA was estimated to be (2.00 ± 0.06) g cm^{-3} directly from its theoretical molecular volume ($V = 126$ Å^3). The value exceeds that of most high energy density materials, such as 1,3,5-trinitro-1,3,5-triazine (RDX; 1.82 g cm^{-3}) and 1,3,5,7-tetranitro-1,3,5,7-tetrazocine (HMX; 1.91 g cm^{-3}), and it rivals that of high-performance oxidizers and explosives, such as ammonium perchlorate (AP; 1.95 g cm^{-3}) and hexanitrohexaazaisowurtzitane (CL-20; 2.05 g cm^{-3}).

$\Delta H^0_{f(gas)}$ of TNA was calculated to be (54.8 ± 2) kcal mol^{-1} by combining highly accurate experimental heats of formations with theoretical reaction energies (see the Supporting Information). Our $\Delta H^0_{f(gas)}$ value is in poor agreement with earlier B3LYP estimates (71 kcal mol^{-1}).[14] The agreement is somewhat better with reported MP2 values (50–65 kcal mol^{-1}).[13,14] The large difference is again explained by B3LYPs overestimation of the TNA ground-state energy. The heat of formation in the condensed phase was estimated to be $\Delta H^0_{f(s)} = (48.4 \pm 5)$ kcal mol^{-1} by subtracting our calculated heat of sublimation, ΔH_{sub}, from $\Delta H^0_{f(gas)}$.

Theoretical performances of hypothetical TNA-based propellants have been compared to similar liquid oxygen (LOX), nitrogen tetroxide (NTO), and AP mixtures (see the Supporting Information). TNA is expected to provide specific impulses (Ns kg^{-1}) that are comparable to all three references when combusting similar fuels. Owing to a higher density, the TNA propellants are expected to enable a roughly 30% higher density impulse (Ns L^{-1}) than LOX, a 16–20% improvement to NTO when combusting hydrogen-rich fuels, and a 19% increase as compared to AP when combusting aluminum. Thus, provided that feasible synthesis and handling of TNA can be managed, it could constitute an environmentally friendly high-performance oxidizer for cryogenic rocket engines.

Two synthetic routes to TNA were considered [Eq. (1) and (2)]. Based on previous theoretical work,[16] the $N(NO_2)_2$ radical can be assumed to be reasonably stable, and it might constitute an intermediate to TNA. The oxidation of $N(NO_2)_2^-$ requires a positive absolute potential of at least 4.4 eV.[19] Thus, electrochemical synthesis of TNA by electrochemical oxidation of $N(NO_2)_2^-$, in the presence of N_2O_4, appears reasonable at low temperatures [Eq. (1)].

A second alternative is direct nitration of $N(NO_2)_2^-$ [Eq. (2)]. The procedure requires a strong nitration agent, which allows the nitronium cation (NO_2^+) to be present in free form. The calculated electrostatic potential of $N(NO_2)_2^-$ reveals that the negative charge is predominantly delocalized over the oxygen atoms.[20] However, the central nitrogen still holds some negative charge, and the greater thermodynamic gain associated with nitrogen addition, in contrast to oxygen addition, should enable a selectivity towards TNA (**1**) ahead of the less stable conformer **4**.

$$N(NO_2)_2^- \xrightarrow{ox} N(NO_2)_2^{\bullet} + e^- \xrightarrow{NO_2^{\bullet}} N(NO_2)_3 \quad (1)$$

$$N(NO_2)_2^- \xrightarrow{NO_2^+} N(NO_2)_3 \quad (2)$$

The second route was chosen, and TNA was obtained by low-temperature nitration of both ammonium dinitramide (ADN) and potassium dinitramide (KDN) in acetonitrile, using NO_2BF_4 as nitration agent. In situ IR spectroscopy was used to follow the reaction from −40 °C up to room temperature (Figure 1). The main IR bands originating from

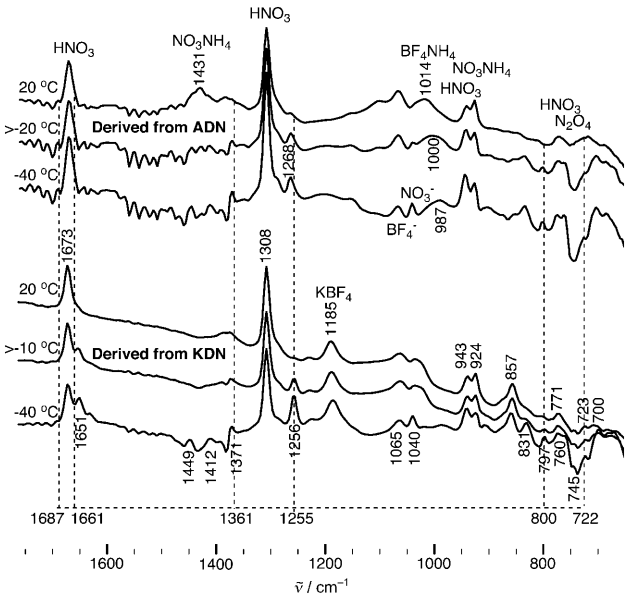

Figure 1. IR spectra of reaction mixtures after subtraction of the acetonitrile background at different temperatures. Theoretical frequencies of TNA are overlaid as dashed lines.

$N(NO_2)_2^-$ (1520, 1188 and 1007 cm^{-1}) disappear when a sufficient amount of NO_2BF_4 is added. Nitric acid (HNO_3) was detected in ample amounts (1673, 1308, and 771 cm^{-1}). This is expected, as any residual water in the reactant solutions would have hydrolyzed NO_2^+.

Six IR bands (1673, 1651, 1371, 1256, 797, and 723 cm^{-1}) appeared, in good agreement with our theoretical estimate for TNA (Figure 1 and Supporting Information). The bands disappeared when the temperature was raised from −40 °C towards room temperature, in good agreement with the theoretical estimates.

TNA was also identified by low-temperature ^{14}N NMR spectroscopy (Figure 2). Natural-abundance ^{15}N NMR spectroscopy did not provide sufficient signal-to-noise ratio. The

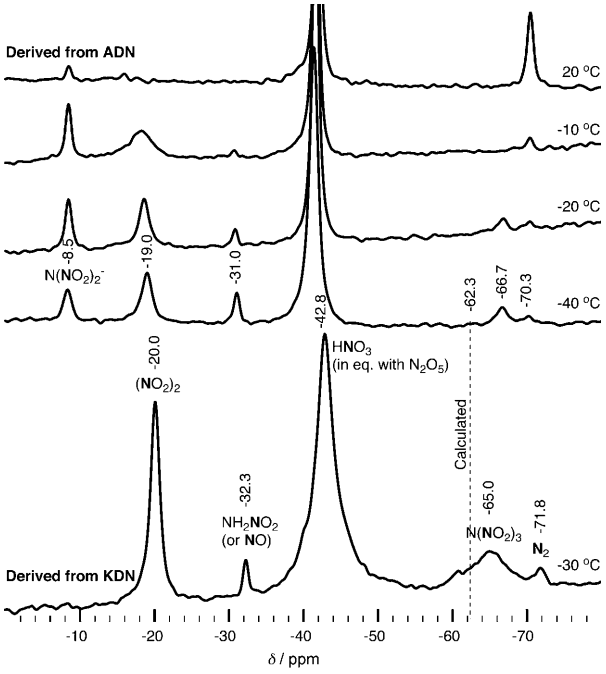

Figure 2. ^{14}N NMR spectra of reaction mixtures at different temperatures. Omitted are higher chemical shifts from acetonitrile (−138 pmm, solvent), N_2O (−146 and −230 ppm), and NH_4^+ (−360 ppm).

nitro groups of TNA were assigned to a peak seen between −66.7 and −64.8 ppm. These values are in good agreement with our theoretical estimate of −62.3 ppm. Aside from being of one-third intensity, the signal of the central nitrogen atom most likely suffers from extensive broadening owing to quadrupolar relaxation;[21] the highest principal value of the electric field gradient tensor is estimated to be almost one order of magnitude larger for central nitrogen than that for the other nitrogen atoms (both for $N(NO_2)_2^-$ and TNA; see the Supporting Information). Thus, the line width of the central nitrogen atom can be two orders of magnitude larger than that for the nitro groups. TNA was seen to decompose when the temperature exceeded approximately −10 °C, in agreement with the IR study. Some HNO_3 (−41.4 ppm) was found already in the NO_2BF_4 reagent solution, where also NO_2^+ was present at −132 ppm. This was expected to be due to the hygroscopic nature of the NO_2BF_4 salt.

After combination of the reagents at low temperature, six resonances appeared. N_2O was seen in large amounts at −147 and −231 ppm. Its existence can be explained by the decomposition of both TNA and $N(NO_2)_2^-$.[16,19,22] A peak at −19 ppm (shift values refer to ADN solutions, shifts in KDN solutions are slightly different) was designated to N_2O_4, in excellent agreement with literature values.[23] This species is also expected to form, through decomposition of both $N(NO_2)_2^-$[16,19,22] and TNA (Scheme 1). In some cases, when extremely dry reagents were used, or when an excess of NO_2BF_4 was added, an HNO_3–N_2O_5 equilibrium was observed between −40 and −55 ppm.

A peak at −31 ppm was identified as NH_2NO_2, in good agreement with both our theoretical estimates (−35.1 ppm) and literature values.[24] The formation of NH_2NO_2 is explained by nitration of ammonia, which could form through proton abstraction from NH_4^+, or from decomposition of $N(NO_2)_2^-$ in the presence of protons. The peak could also correspond to some sort of unstable NO complex, as previously suggested.[25] N_2 was found at −71 ppm.

The nitro groups of $N(NO_2)_2^-$ were observed at −8.5 ppm, in good agreement with previous measurements.[26] The stability of $N(NO_2)_2^-$ is reduced in the very harsh environment, and it was seen to slowly decompose into HNO_3, N_2O_4, and N_2O above a temperature of approximately 0 °C.

The peaks designated to NH_2NO_2 (or NO) and N_2O_4 disappeared above −10 °C. This also in agreement with literature, which has shown that NH_2NO_2 under acidic conditions decomposes to HNO_3 above −5 °C.[27] N_2O_4 is likely dissociated into NO_2 at higher temperatures (or could also be oxidized or hydrolyzed).

To summarize, we have subjected TNA to an extensive theoretical investigation that led to its detection at low temperature by IR and NMR spectroscopy. The molecule is by far the largest nitrogen oxide known, and it is predicted to have excellent properties as an oxidizer for cryogenic propulsion.

Experimental Section

Caution! Several of the used and investigated compounds are highly energetic. They should be handled on a small scale while using appropriate safety precautions, such as a face shield, leather gloves, and protective clothing.

Materials: Acetonitrile (anhydrous, ≥99.8%, Sigma–Aldrich), NO_2BF_4 (≥95.0%, Fluka), 2-propanol (99.8%, Scharlau), diethyl ether (99.9%, Prolabs); ammonium dinitramide (ADN; batch ADN-0546172, ≥99.2%) and potassium dinitramide (KDN; batch KDN-502, >99.5%) were kindly supplied by Eurenco Bofors. ADN (1.0 g) was dried by dissolving in methanol (1.6 mL), filtering, and precipitating in cold (< −20 °C) diethyl ether (100 mL). KDN (1.1 g) was dried by dissolving in distilled water (2 mL), filtering, and precipitating in cold (< −20 °C) 2-propanol (100 mL). Both solids were stored at 50 °C during the 48 h before use.

Nitration of dinitramide salts, method 1: NO_2BF_4 (53.2 mg, 0.4 mmol, partly hydrolyzed) was sealed in a glass vial under argon and dissolved in cold (ca. −20 °C) and dry acetonitrile (2 mL, 0.2 M). ADN (24.8 mg, 0.2 mmol) and KDN (29 mg, 0.2 mmol) were each dissolved in dry acetonitrile (1 mL, 0.2 M) and kept under argon. In a

typical experiment, either of the dinitramide solutions was lowered into an acetonitrile/CO_2(s) cold bath (−40 °C). NO_2BF_4 solution (1 mL) was then added by slow dropwise addition with stirring. The reaction to form TNA was instantaneous.

Nitration of dinitramide salts, method 2: To limit the exothermicity associated with method 1 (which can result in low or no yield), pure NO_2BF_4 was added directly to frozen solutions of ADN and KDN. Subsequent slow dissolution of NO_2BF_4 at −40 or −30 °C provided better thermal control.

^{14}N NMR: (36.1 MHz, −40 °C, acetonitrile): $\delta = -66.8$ to −64.8 ppm (s, 3N, $N(NO_2)_3$). IR: (acetonitrile, −40 °C): $\tilde{\nu} = 1673$ (s), 1651 (s), 1371 (w), 1256–1263 (s), 797 (w), 723 (w) cm^{-1}.

Apparatus: ^{14}N NMR spectra were acquired on a Bruker 500 Avance III spectrometer. The chemical shift scale was referenced by setting the frequency of 0.2 M nitromethane in acetonitrile to zero ppm at −40 °C. Up to four thousand transients were accumulated with a repetition time of 1 s. IR measurements were made on a ReactIR iC10 from Mettler Toledo equipped with a SiComp probe using the iC IR software. One spectrum (256 scans) was measured per minute.

Computational details: Reported relative energies were calculated using CBS-QB3[28] in Gaussian 03.[29] Solvation energies were obtained at the COSMO-B2PLYP[30]/aug-cc-pVTZ//PCM-B3LYP/6-31 + G(d) level using the ORCA[31] program.[19] The density of TNA was obtained from the volume of its 0.001 a.u. electron density contour using a B3LYP/6-31G(d) wavefunction and the HS95-v09[32] program. ΔH_{vap} and ΔH_{sub} were obtained from the calculated electrostatic potential (ESP) at the same level, using a parameterization relationship.[33] $\Delta H^{0}_{f(gas)}$ was obtained from an average of three CBS-QB3 reaction enthalpies combined with experimental data. Nuclear magnetic shielding tensors were calculated in acetonitrile at the GIAO-PCM-B3LYP/6-311 + + (3df,3pd) level. IR spectra in acetonitrile were calculated at the PCM-B3LYP/6-31 + G(d) level and scaled by 0.972 for best fit with experimental results. Rocket-propellant performance was calculated using the NASA CEA code.[34] More information is given in the Supporting Information.

Received: November 9, 2010
Published online: December 23, 2010

Keywords: energetic materials · nitrogen oxides · propellants · quantum chemistry · trinitramide

[1] J. Giles, *Nature* **2004**, *427*, 580 – 581.
[2] R. P. Singh, R. D. Verma, D. T. Meshri, J. M. Shreeve, *Angew. Chem.* **2006**, *118*, 3664 – 3682; *Angew. Chem. Int. Ed.* **2006**, *45*, 3584 – 3601.
[3] M. B. Talawar, R. Sivabalan, T. Mukundan, H. Muthurajan, A. K. Sikder, B. R. Gandhe, A. S. Rao, *J. Hazard. Mater.* **2009**, *161*, 589 – 607.
[4] K. O. Christe, W. W. Wilson, J. A. Sheehy, J. A. Boatz, *Angew. Chem.* **1999**, *111*, 2112 – 2118; *Angew. Chem. Int. Ed.* **1999**, *38*, 2004 – 2009.
[5] R. Haiges, S. Schneider, T. Schroer, K. O. Christe, *Angew. Chem.* **2004**, *116*, 5027 – 5032; *Angew. Chem. Int. Ed.* **2004**, *43*, 4919 – 4924.
[6] T. M. Klapötke, J. Stierstorfer, *J. Am. Chem. Soc.* **2009**, *131*, 1122 – 1134.
[7] A. Vij, J. G. Pavlovich, W. W. Wilson, V. Vij, K. O. Christe, *Angew. Chem.* **2002**, *114*, 3177 – 3180; *Angew. Chem. Int. Ed.* **2002**, *41*, 3051 – 3054.
[8] H. Östmark, S. Wallin, T. Brinck, P. Carlqvist, R. Claridge, E. Hedlund, L. Yudina, *Chem. Phys. Lett.* **2003**, *379*, 539 – 546.
[9] O. A. Luk′yanov, Y. V. Konnova, T. A. Klimova, V. A. Tartakovsky, *Izv. Akad. Nauk Ser. Khim.* **1994**, 1264 – 1266.
[10] J. C. Bottaro, P. E. Penwell, R. J. Schmitt, *Synth. Commun.* **1991**, *21*, 945 – 949.
[11] R. Gilardi, J. Flippen-Anderson, C. George, R. J. Butcher, *J. Am. Chem. Soc.* **1997**, *119*, 9411 – 9416.
[12] E. A. Miroshnichenko, L. I. Korchatova, B. L. Korsunskii, B. S. Fedorov, Y. D. Orlov, L. T. Eremenko, Y. A. Lebedev, F. I. Dubovitskii, *Dokl. Akad. Nauk SSSR* **1987**, *295*, 419 – 423.
[13] J. A. Montgomery, Jr., H. H. Michels, *J. Phys. Chem.* **1993**, *97*, 6774 – 6775.
[14] Z. Chen, T. P. Hamilton, *J. Phys. Chem. A* **1999**, *103*, 11026 – 11033.
[15] A. I. Kazakov, Y. I. Rubtsov, G. B. Manelis, L. P. Andrienko, *Russ. Chem. Bull.* **1997**, *46*, 2015 – 2020.
[16] M. Rahm, T. Brinck, *J. Phys. Chem. A* **2010**, *114*, 2845 – 2854.
[17] J. S. Murray, T. Brinck, P. Politzer, *Chem. Phys.* **1996**, *204*, 289 – 299.
[18] P. Politzer, J. S. Murray, *J. Phys. Chem. A* **1998**, *102*, 1018 – 1020.
[19] M. Rahm, T. Brinck, *Chem. Eur. J.* **2010**, *16*, 6590 – 6600.
[20] J. P. Ritchie, E. A. Zhurova, A. Martin, A. A. Pinkerton, *J. Phys. Chem. B* **2003**, *107*, 14576 – 14589.
[21] J. Kowalewski, Mäler, L., Nuclear Spin Relaxation in Liquids: Theory, Experiments, and Applications, Taylor and Francis, New York, **2006**.
[22] M. Rahm, T. Brinck, *Chem. Commun.* **2009**, *20*, 2896 – 2898.
[23] X. Zhang, K. Seppelt, *Z. Anorg. Allg. Chem.* **1998**, *624*, 667 – 670.
[24] A. Haussler, T. M. Klapötke, H. Piotrowski, *Z. Naturforsch. B* **2002**, *57*, 151 – 156.
[25] V. M. Mastikhin, S. V. Filimonova, *J. Chem. Soc. Faraday Trans.* **1992**, *88*, 1473 – 1476.
[26] V. A. Shlyapochnikov, M. A. Tafipolsky, I. V. Tokmakov, E. S. Baskir, O. V. Anikin, Y. A. Strelenko, O. A. Luk′yanov, V. A. Tartakovsky, *J. Mol. Struct.* **2001**, *559*, 147 – 166.
[27] A. A. Lobanova, S. G. Il′yasov, N. I. Popov, R. R. Sataev, *Russ. J. Org. Chem.* **2002**, *38*, 1 – 6.
[28] J. A. Montgomery, Jr., M. J. Frisch, J. W. Ochterski, G. A. Petersson, *J. Chem. Phys.* **1999**, *110*, 2822 – 2827.
[29] Gaussian 03 (Revision C.02), M. J. Frisch, et al., Gaussian, Inc. Wallingford, CT, **2004**. See S. I. for full list of authors.
[30] S. Grimme, *J. Chem. Phys.* **2006**, *124*, 034108.
[31] F. Neese, T. Schwabe, S. Grimme, *J. Chem. Phys.* **2007**, *126*, 124115.
[32] T. Brinck, Hardsurf program. (HS95v09), **2009**.
[33] B. M. Rice, S. V. Pai, J. Hare, *Combust. Flame* **1999**, *118*, 445 – 458.
[34] B. J. McBride, S. Gordon, *Computer Program for Calculation of Complex Chemical Equilibrium Compositions and Applications. II. Users Manual and Program Description*, NASA, **1996**.

